

Axial Response of Resin Encapsulated Cable Bolts in Monotonic and Cyclic Loading

Ashkan Rastegarmanesh*¹, Ali Mirzaghobanali², Kevin McDougall², Naj Aziz³, Sina Anzanpour³, Hadi Nourizadeh¹, Mahdi Moosavi⁴

Abstract

The ease of use and the design flexibility of cable bolts have made them a popular choice for rock support. Cable bolts can be encapsulated with cementitious grout or resin. There is a need to better understand the impact of resins on the behaviour of cable bolts under varying load and stress regimes over their long service life. This study reports on 18 large scale resin pull out tests. The testing apparatus minimised the rotational movement of the cable at the exit point by using a fully grouted anchor tube. Six cable bolts, ranging from 50 to 100 tonnes in capacity, anchored using a fast-curing urea silica resin, were tested under monotonic and cyclic loading. Each cable type was tested twice in monotonic loading and then the average initial peak load was used to generate a cyclic loading pattern. The study found that the resin product had a relatively low load capacity regardless of the cable type, and that loading type had a minimal impact on the results. The cable diameter had a minor influence on the pull out results. The resin provided a stiff behaviour and an excellent response to repeated loading.

Keywords: Cable bolts, Pull out, Resin, Cyclic

1 Centre for Future Materials, University of Southern Queensland, Toowoomba, Australia (Corresponding author) Rastegarmanesh@gmail.com

2 School of Civil Engineering and Surveying, University of Southern Queensland, Toowoomba, Australia

3 School of Civil, Mining & Environmental Engineering, University of Wollongong, Wollongong, Australia

4 School of Mining Engineering, University of Tehran, Tehran, Iran

1 Introduction

Cable bolts and rock bolts are one of the most widely used forms of underground support in mining and civil projects. Over time, cable bolt technology has matured, and many different types of cable bolts have been developed to suit a variety of applications. As illustrated in the catalogue of bolt companies (e.g., Jennmar Australia, 2020), cable bolts now have various diameters, load capacities, surface profile configurations, bulb structures, and central hole configurations.

1.1 Bonding Agent

Various bonding agents have been used for tendon installation in both mining and civil projects. Traditionally, conventional cement paste was used to fix bolts into the strata. Plain cement cures slowly and shrinks, and its exposure to groundwater can cause it to eventually break down, exposing the support element to corrosion. As a result, special cementitious grouts (e.g., thixotropic grouts) were developed by adding various additives to the cement powder to make it stronger, faster setting, more pumpable, and non-shrinking (Aziz *et al.*, 2017; Meikle *et al.*, 2013). The use of these cementitious products became extremely widespread and the cornerstone of rock bolting and cable bolting.

While these special grouts addressed many of the shortcomings of conventional cement, they were still cementitious in nature, which meant having a gentle curing curve and being susceptible to water corrosion over time (Kilic *et al.* 2002). Consequently, resin products have gained popularity in the anchoring industry due to their fast curing time and resistance to corrosion.

Rasekh (2017), after Tadolini (2016), estimated that in 2011, out of the 100 million roof bolts used in US mines, 66% were bonded with resin and 9% were resin-reinforced bars.

However, resins are often more expensive, less environmentally friendly, more complex to utilize, and most importantly increase the chance of uneven encapsulation when used for the full length of the tendon due to their fast curing time, poor mixing potential, and gloving (Villaescusa *et al.* 2008).

1.2 Pull out Tests

In the axial test, the encapsulated cable is pulled out of a confining medium which can be in the form of a metal pipe, concrete, rock, or a combination of these (Fuller and Cox, 1975; Hutchins *et al.*, 1990; Reichert, 1991; Clifford *et al.*, 2001; Thomas, 2012). As the

strength and stiffness of the confining medium affect pull out load, various methods (e.g., biaxial cell) were proposed to maintain constant normal stiffness or pressure conditions (MacSporran, 1993; Hyett *et al.*, 1995; Hyett *et al.*, 1996; Moosavi *et al.*, 1996). Today's higher-capacity cables require testing apparatuses that can support higher loads.

Hawkes and Evans (1951) were among the first to study resin-anchored columns in pull out testing and proposed an exponential model for load distribution along the bolt. Craig and Holden (2014) used the Laboratory Short Encapsulation Pull Test (LSEPT) and Single Embedment Pull Test (SEPT) setup to study resin-encapsulated cables in both lab and field conditions, and concluded that the resin's fast curing time resulted in higher load capacity over a shorter time frame. Chen *et al.* (2016) and (2018) utilized a Modified LSEPT to study various aspects of cable bolt pull out tests. The setup included artificial rocks encapsulating plain and bulbed cables.

Martin (2012) examined five resin-anchored cable bolts with different encapsulation lengths in a biaxial pressure cell with respect to unscrewing, and concluded that the resin was damaged even when rotation was allowed during the test. Bajwa *et al.* (2017) compared resin and grout products' performance in pull out tests and reported that, in smaller boreholes, grout had a better performance for a plain smooth cable, while in the larger boreholes, resin provided higher load with lower repeatability.

While pull out tests provide an accurate measure of the overall performance of the system (cable, bonding annulus, and the confining medium), they tend to overlook some other aspects of the design. For instance, normal pull out tests focus on the maximum loading capacity of a cable under monotonic loading even though most cable bolts never reach their ultimate load in the field. The complex environment of underground mines typically involves frequent blasting, heavy machinery operations, excavation and backfilling in the hanging wall, and seismicity such as quakes or rockbursts. These phenomena can change the stress regime of an in-situ cable quite significantly through multiple stressing and destressing cycles. Therefore, it is critical to investigate the cable bolts' service life performance in various loading patterns. A cyclic testing pattern to replicate the loading and unloading can provide some further evidence of the performance of bonding agents, such as resins, during axial loading.

As far as can be determined, there are limited systematic research studies on the axial load transfer mechanisms of cable bolts encapsulated by resin under monotonic and cyclic loading. Most previous studies (i.e. Villaescusa *et al.*, 2008; Aziz *et al.*, 2016; Thenevin *et al.*, 2017; Salcher and Bertuzzi, 2018) either focus on rock bolts/bars, or resin types mainly designed for rock bolting which typically vary in characteristics from cable bolting resins.

This paper addresses this gap in knowledge by testing three resin-encapsulated samples of six different cable types (a total of 18 samples) in a series of pull out tests under both “conventional monotonic” and “cyclic” loading scenarios.

A newly designed MSEPT (Modified Single Embedment Pull Test) with anti-rotational 1000 kN pull out capacity was manufactured and utilised as the testing apparatus. Each cable was tested three times using a urea silica pumpable resin (Carbothix – Minova) used in the Australian mining industry for cable bolting. The following sections discuss the experimental design, the results achieved and the conclusions drawn.

2 Experimental Concept

Due to the increased capacities of cable bolts, a high-capacity 1000 kN pull out apparatus was designed and manufactured for the testing (Figure 1). The design takes inspiration from the Modified LSEPT utilised by Hagan and Chen (2015) where the cable is encapsulated inside a confined artificial rock cylinder and pulled using a hydraulic jack. A series of modifications were made to this design to improve its capacity and reduce operational costs.

Firstly, the new design comprises a barrel and wedge assembly to carry the load from the hydraulic jack to the cable bolt. This is closer to the field pull out test, is considerably less costly and time-consuming to undertake testing and requires significantly less preparation. The apparatus enables the testing of the newer heavier cables (such as 1000 kN) up to the failure capacity of the barrel and wedge. As barrel and wedge requires an initial load (displacement) to fully lock into place, a separate displacement gauge was installed to record the barrel versus cable displacement throughout the test which could then be subtracted from the ram displacement.

Secondly, as shown in Figure 1, in the free section of the cable bolt an anchor tube is fixed in place with bonding agents. This 300 mm long, 50 mm wide and 4.5 mm thick anchor tube has a 100 mm long key welded onto it that slides inside a slotted guide extruding from the concrete base plate. This plate is also rotationally constrained by an external confinement split pipe grouted to the concrete sample. Through this design, the whole system of external confinement, base plate, anchor tube, and cable bolt is locked together, so the relative rotational movement of these parts is restricted during the pull out.

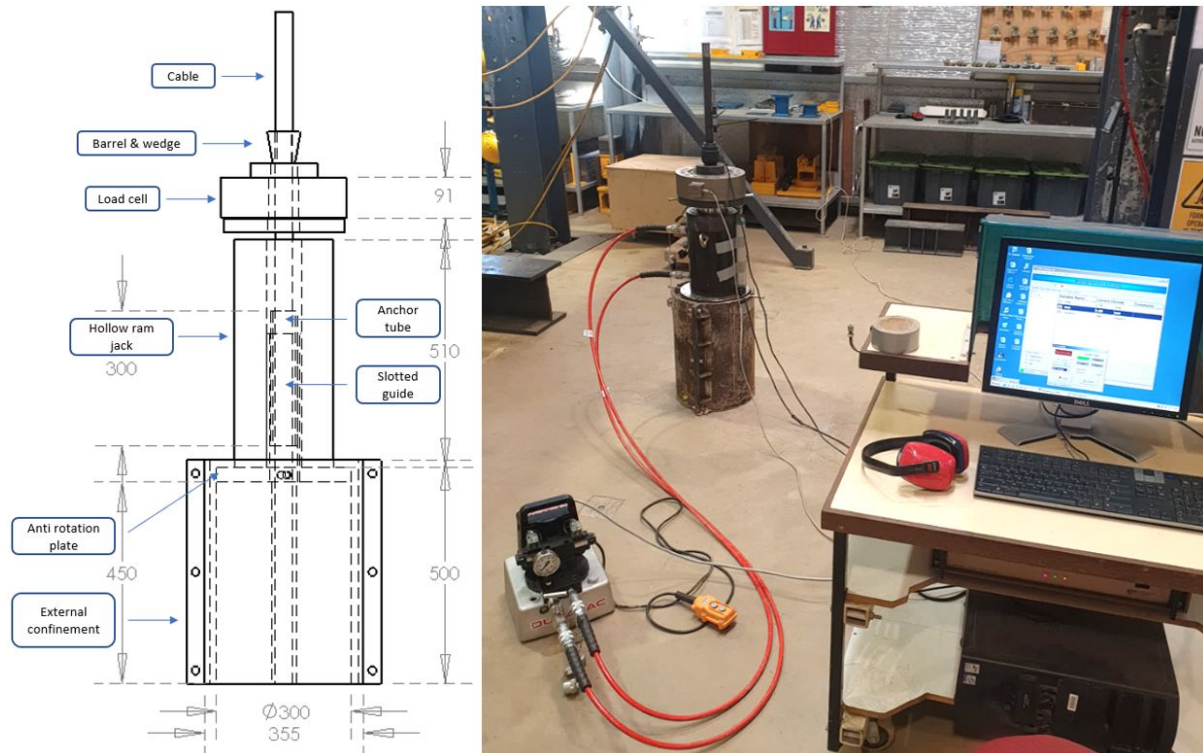


Figure 1 The 1000 kN pull out apparatus design (left) and the test components on the right including the datalogger, low-speed pump, and assembled sample

2.1 Sample Preparation

2.1.1 Cable Bolt Selection

Cable bolts come in a variety of shapes and configurations. In this study, six cable bolts were chosen based on their wide use in the Australian mining industry (Figure 2, Figure 3, and Table 1). The selection of cable bolts covered a series of modifications commonly used, such as “surface” modification (indentations) and “structure” modification (bulbing). The cables were divided into two main categories of “plain” and “bulbed” cables. A *bulbed* cable possesses a structural modification that results in an enlargement (bulb) along the cable. A *plain* cable can be categorised as either *smooth* or *indented*, with an indented cable having surface modifications such as small patterns (indentations). As shown in Table 1, three of the cables were bulbed while the remaining three were plain with one of these cables being indented.

The testing of Superstrand and indented Superstrand cables provided the opportunity to compare the effect of surface indentation in the same cable with differing surface finishes. The testing of the Goliath and plain Superstrand cables enabled a comparison of plain cables of different diameters. Finally, three different size bulbed cables with various

diameters and lay angles provided substantial data on the performance of bulbed cables in the field.



Figure 2 Cable bolts: a) Indented (ID) Superstrand, b) 9 strand, c) 10 strand, d) Goliath, e) 12 strand, and f) Superstrand

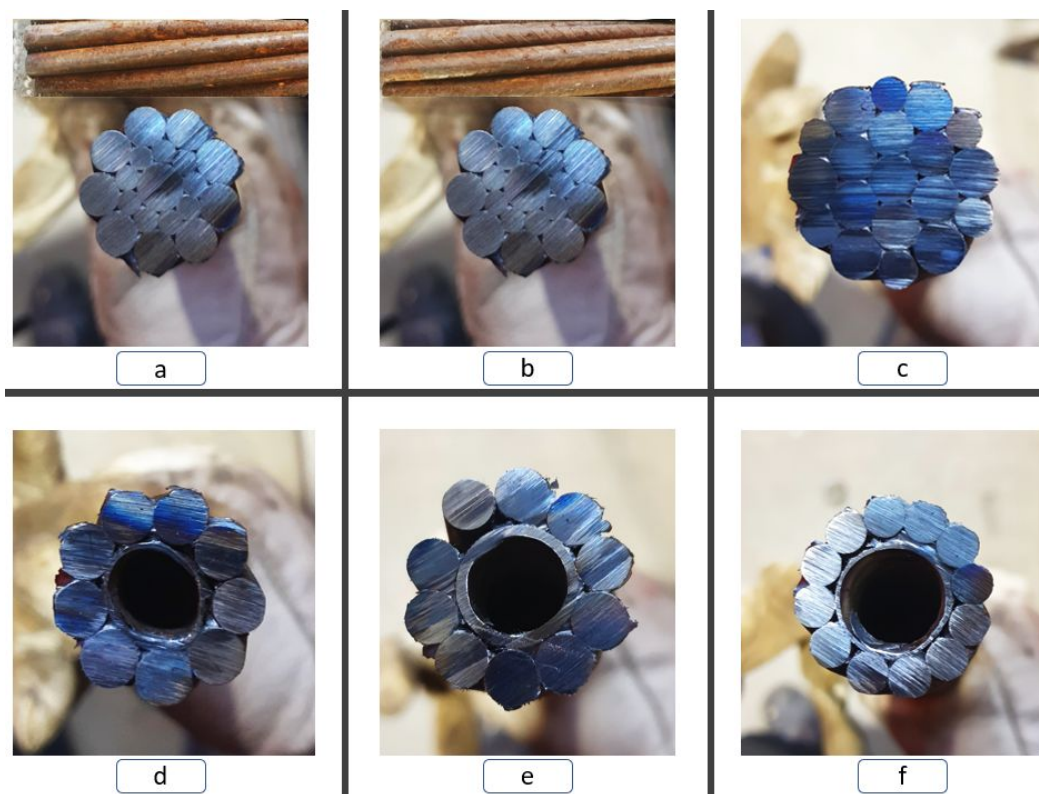


Figure 3 Cable cross-sections – a) Superstrand, b) Indented Superstrand, c) Goliath, d) 9 strand SUMO, e) 10 strand SUMO, and f) 12 strand SUMO (Rastegarmanesh et al. 2022)

Table 1 Cables' specification (Jennmar Australia 2020)

Cable Type	Code	Strand Diameter (mm)	Breaking point @Strands (kN)	Breaking Point @B&W (kN)	Steel Area (mm ²)	Elongation at Failure (%)	Bulb Diameter (mm)	Borehole Diameter (mm)
Goliath	Gol	28.6	970	>800	532	5-7	-	55
12 strand	12S	31	705	640	-	5-7	36	55
10 strand	10S	31	705	640	-	5-7	36	55
9 strand	9S	28	635	540	-	5-7	35	55
Superstrand	SS	21.8	590	520	313	6-7	-	42
Indented Superstrand	IDS	21.8	570	450	313	6-7	-	42

2.1.2 Confinement Medium

Instead of rock, a general-purpose concrete mix was chosen for the confinement medium for ease of use and repeatability. The 28 days UCS test revealed 40 MPa concrete strength. A series of 450 mm long cylindrical “column frameworks” with an internal diameter of 300 mm were cut to create the concrete mould. Based on the manufacturer’s recommendations, two different borehole sizes were created inside each mould using centrally placed 42mm and 55 mm PVC pipes. These PVC pipes were wrapped using a 5 mm ethernet cable with a 25 mm spacing. Upon extraction of the PVC pipe in the later part of the sample preparation process, these cables created a rifling effect similar to the drill bit used in mines (Figure 4). This is important as it minimises the chance of system failure on the grout/concrete interface, biasing a cable/resin interface failure.



Figure 4 Creating internal rifling on the borehole wall

2.1.3 Resin Casting

The cables were centred inside the internally rifled boreholes using a special closed-cell foam. The first 150 mm of the cables were tightly wrapped with the said foam to stop the resin flow to the end of the hole and provide a clean cable section to be fed through during the test. Without this measure, the encapsulation length would shorten as the cable is pulled out during the tests. Carbothix Fast (Minova), a urea silica fast-set resin popular for cable bolting in Australia, was used (Table 2). Carbothix requires a special-purpose compressed air pump for mixing and injection due to its 1:1 mixing ratio, high-temperature exothermic reaction (+100 Celsius), and super-fast curing time (15 seconds). Figure 5 illustrates different stages of sample preparation.

Table 2 Material data for Carbothix (Minova 2020)

Parameters	Unit	Component A	Component B	Standard
Density at 25 °C	Kg/m ³	1450 ± 50	1160 ± 50	DIN 12791-1
Colour	-	Brownish	Dark Brown	-
Flash point	°C	n.a.	> 100	EN ISO 1523
Viscosity at 25 °C	mPa*s	360 ± 60	190 ± 40	DIN EN ISO 3219

Next, the 300 mm internally rifled anchor tubes were secured and centred around the cable bolts, 100 mm above the concrete surface. This gap although not ideal, was functional and provided a lifting point for the heavy samples. This gap also provided enough space to add grout to the top of the concrete samples in the next stage to compensate for some unevenness of the concrete surface, avoid stress concentration, and provide even surface confinement. In the final test assembly, this length was approximately 50 mm. The anchor tubes were also anchored with the same product. Under normal field conditions, the space between the hypothetically two separating beds or rock blocks is almost never this large.

The outcome of sample preparation was a concrete sample 450 mm long with the first 150 mm from the bottom of the cable not encapsulated due to the closed cell foam. Therefore, the resin column was 300 mm long with the centre of the bulbed cables located at 100 mm from the bottom (entry point) and 200 from the top (exit point/collar).



Figure 5 Sample preparation

2.2 Resin Properties

Six 50 mm cubic resin samples were cast according to the British Standard for grout testing. The samples were tested using a strain-control compression machine and the data was recorded using a Digital Image Correlation (DIC) camera. Figure 6 and Table 3 summarise the results. Carbothix showed a strain hardening behaviour with often unclear failure points and mostly barrel shape failure. Where the samples were completely disintegrated, no visible yield point was observed, however, load kept increasing. As a result, the yield point and relevant values were extracted based on a proposed 2% offset rule.

This method, essentially adopted after the 0.2% method used for certain materials that don't exhibit distinct failure points, assumes the intersection of the uniaxial compression graph with an arbitrary line starting from 2% strain on the horizontal axis and parallel to the secant elastic modulus with respect to the first major deflection point, as the yield point of the sample.

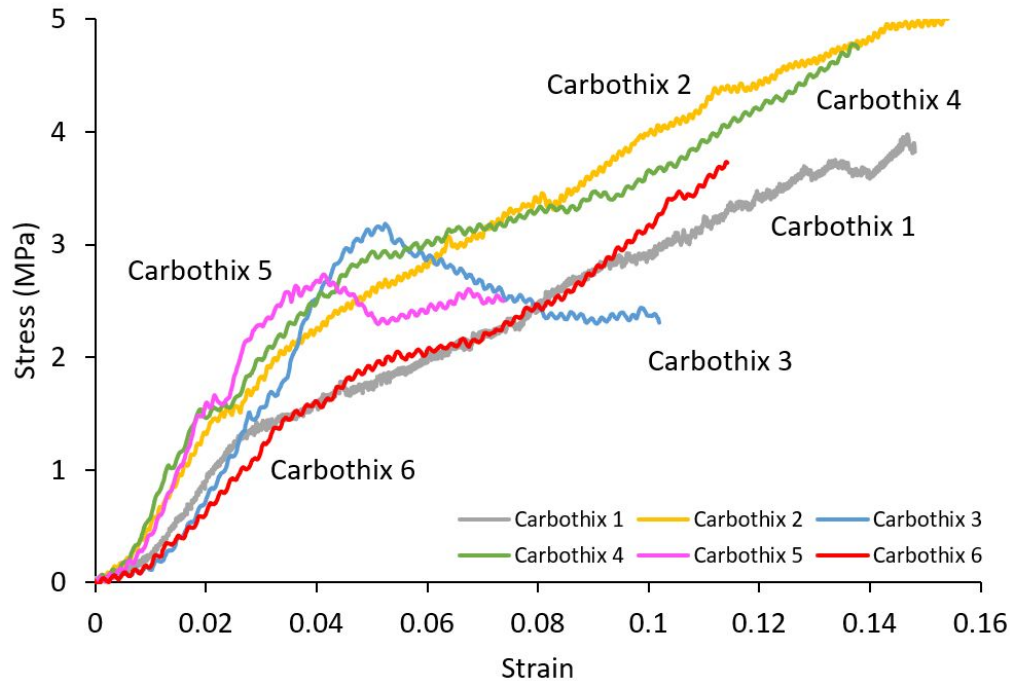


Figure 6 Carbothix stress-strain graph

Table 3 Carbothix mechanical properties

Sample	Yield Stress (MPa)	Initial Young's Modulus (MPa)	Secant Young's Modulus (MPa)
Carbothix 1	1.68	44.50	38.18
Carbothix 2	2.64	65.33	50.77
Carbothix 3	2.89	40.95	57.80
Carbothix 4	2.72	70.83	60.44
Carbothix 5	2.71	65.38	66.10
Carbothix 6	2.01	37.20	40.20
Carbothix (avg)	2.44	54.03	52.25
Std Dev	0.44	13.44	10.29

2.2.1 Testing Procedure

Each sample was placed in a 330 mm diameter, 12 mm thick, split pipe as external confinement (Figure 7 - left). The split pipe was closed using six high-strength bolts (12.9 grade) and torqued to 80 Nm. The gap between the sample exterior (300mm) and the internal surface of the external confinement (330 mm) was filled with a 0.4 W:G ratio mix of cementitious grout (Stratabinder – Minova). Each sample was left 48 hours to cure to enable the filler grout to reach approximately the same UCS as the concrete (40 MPa).

On the testing day, the anti-rotation base plate was lowered to the top of the concrete sample followed by the 100-tonne hollow ram jack. Next, the load cell assembly containing a base plate and top (reaction) plate was placed on the jack's saddle. Finally, the whole

system was topped with each cable's barrel and wedge and then the wedges were hammered into the barrel to initialize the barrel and wedge.

A 225 mm stroke spring-loaded LVDT (linear variable differential transformers) was fixed to the side of the hydraulic jack to measure the total vertical movement of the system. A 100 mm stroke spring-loaded LVDT was secured to the free end of the cable, while resting on the barrel, to measure the amount of displacement it took for the barrel to lock into place (Figure 8 right). The subtraction of these two displacements was the pure pull out length of the cable (assuming the elastic axial strain of the cable is negligible).

The jack was used with a slow-speed hydraulic power unit, providing an average rate of vertical displacement of 6 mm per minute. Finally, the two LVDTs, the hydraulic ram, and the 1000 kN load cell were all connected to a data logger with a 10 Hz recording rate. Each test was continued to at least 120 mm of vertical displacement to provide adequate information about the post-peak (residual) behaviour. Each cable type was tested twice in monotonic loading and then the average initial peak load was used to generate a cyclic loading pattern of five equally spaced ascending steps to be tested on the third sample.



Figure 7 Left: External confinement, and right: Instrumentation and testing components

3 Results

Monotonic loading describes a loading function with the intention of a decreasing or increasing path until failure (e.g., conventional compression/tension tests). On the other hand, cyclic loading in this study is defined as a loading path in which multiple increasing loading steps are applied with unloading steps in between. This was undertaken using the average maximum load from the monotonic tests as a benchmark, The average value was then divided by five to establish the loading steps.

In the first step, $1/5$ of the load was applied, followed by unloading. In each following step, the load was increased by a factor of $1/5$ (e.g., $1/5$, $2/5$, $3/5$, $4/5$ and $5/5$). After each loading step, unloading was performed. In the last step, the whole monotonic load ($5/5$) was applied, and the test was continued until 120 mm of vertical displacement was achieved.

Based on the coding convention from Table 1, the individual cable bolt samples are denoted hereon by their code for brevity. For instance, SS(1) is the “first” sample of the “monotonic” test of “Superstrand” and SS(2) is the “second” “monotonic” test sample. The prefix (C) indicates the sample results for the “cyclic” loading test, while the suffix (#) denotes the curves that are “denoised”. The denoising procedure is detailed later on.

The detailed graphs of the cyclic and monotonic loading comparisons are presented in the supplementary data. The findings of the experimental plan are summarised in Figure 8. Almost all cables showed similar behaviour, with an initial drop of load after the peak, and then a plastic or strain-hardening behaviour in the post-peak area (residual). This was particularly prominent in the Goliath (Gol), 9 strand (9s), and 12 strand (12s) cable, hence the two displacements at failure in Figure 8.

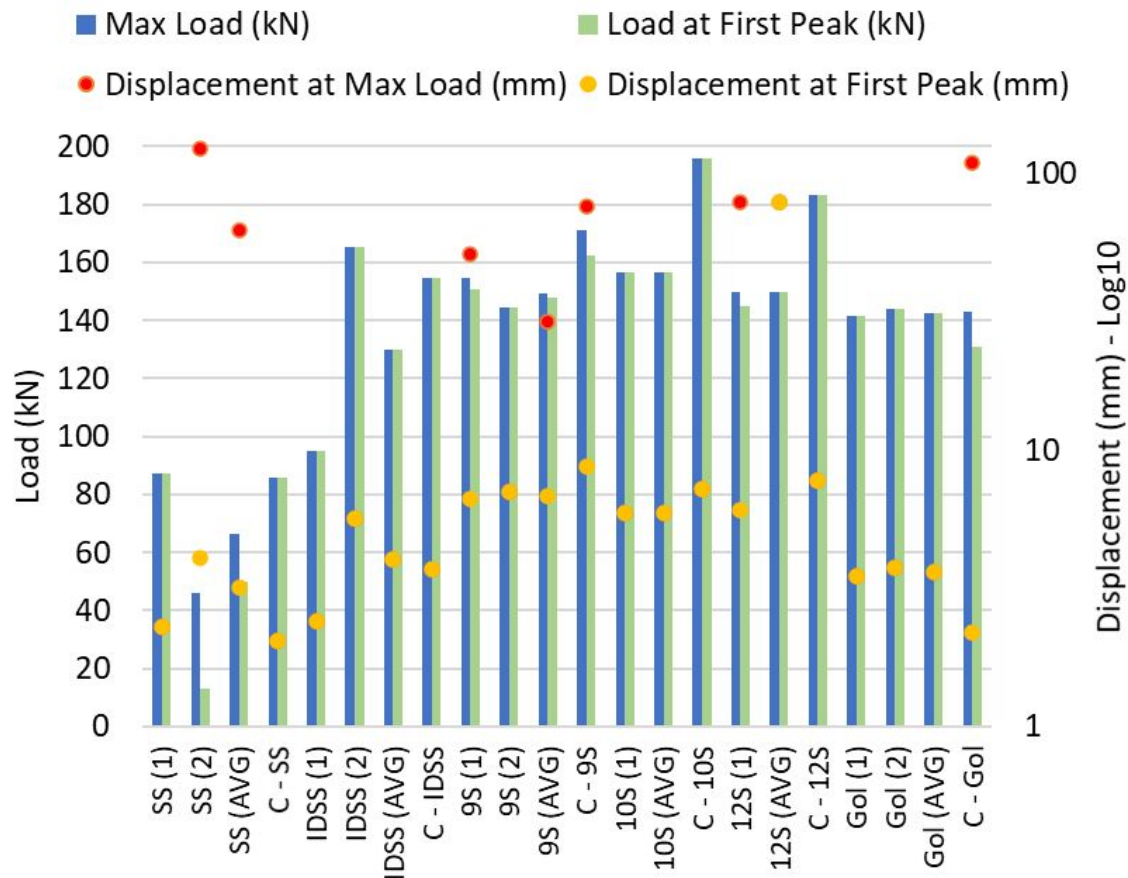


Figure 8 Resin results summary: The displacement axis on the right is logarithmic to fit the large values

3.1 Monotonic Testing

As seen in Figure 8, comparing the results of the Superstrand, IDSuperstrand and Goliath (the plain cables) with 9, 10, and 12 strand cables (the bulbed cables) shows that the bulbed cables recorded a higher average maximum load when compared to the unbulbed cables (Figure 9 and Figure 10). Even when the lower results of the Superstrand are not included, the bulbed cables reached a higher average maximum load. The unwieldy nature of the bulb and its overall shape and dimension exerts significant radial pressure on the resin annulus. The path of least resistance for the bulbs is the destruction of the resin annulus which translates to a higher pull out load compared to the unbulbed cables where the strands can mostly travel inside their respective lug inside the annulus. After all, bulbs are designed to break continuity along the cable.

The bulbed cables also showed consistently higher load with little variation between the samples tested under monotonic loading. This aligns with similar pull out tests on cementitious grout anchored samples (e.g., Chen 2016 and Rastegarmanesh *et al.* 2022) in which the bulbed cables had a considerably higher load capacity. Among the cable

parameters (e.g., diameter, bulb, surface indentation, number of strands, etc.), the load tended to be slightly correlated with the diameter of the cable. This indicates that the Superstrand cables (smooth or indented) could be categorised in a lower load range compared to the bulbed cables. The Goliath (another unbulbed cable) compared favourably to the bulbed cable load range. This indicates that the cable diameter, and therefore the contact surface area of the resin, has an impact.

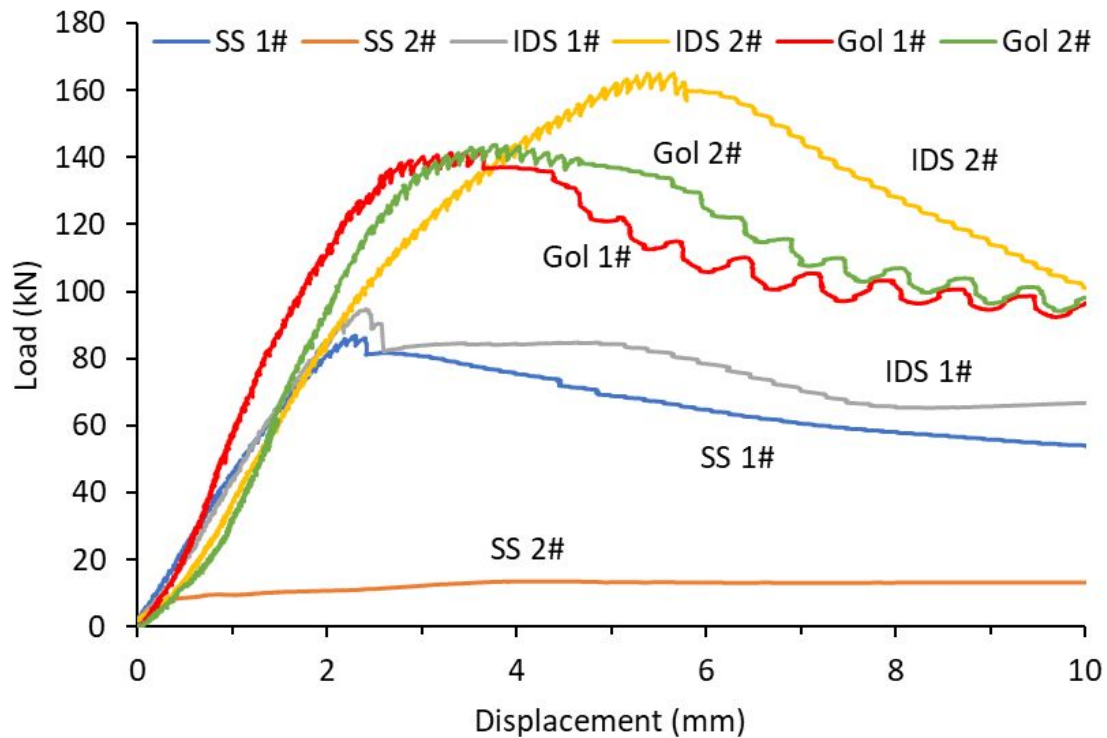


Figure 9 Pre-peak monotonic results of the SS, IDS, and Gol plain cables

The comparison between Superstrand and indented Superstrand emphasises the impact of surface indentation on the overall load capacity of the cable bolts (Figure 9). However, the four tests on the Superstrand cables (smooth and indented) were inconclusive, with around 50% difference in the load observed between two identical samples. This suggests the sensitivity of these cables to inconsistencies and errors of large-scale testing, as they both have a much smaller surface area.

In addition, observations suggested the resin had difficulty in fully encapsulating these cables compared to thicker ones. This is believed to be due to the smaller cross-sectional area for resin flow between the cable and the borehole. This area has significance as it can cause pressurization, therefore higher encapsulation quality. In smaller cables, a gap can cause lower resin velocity in the hole leading to resin hardening before fully encompassing the full length of the cable (uneven encapsulation).

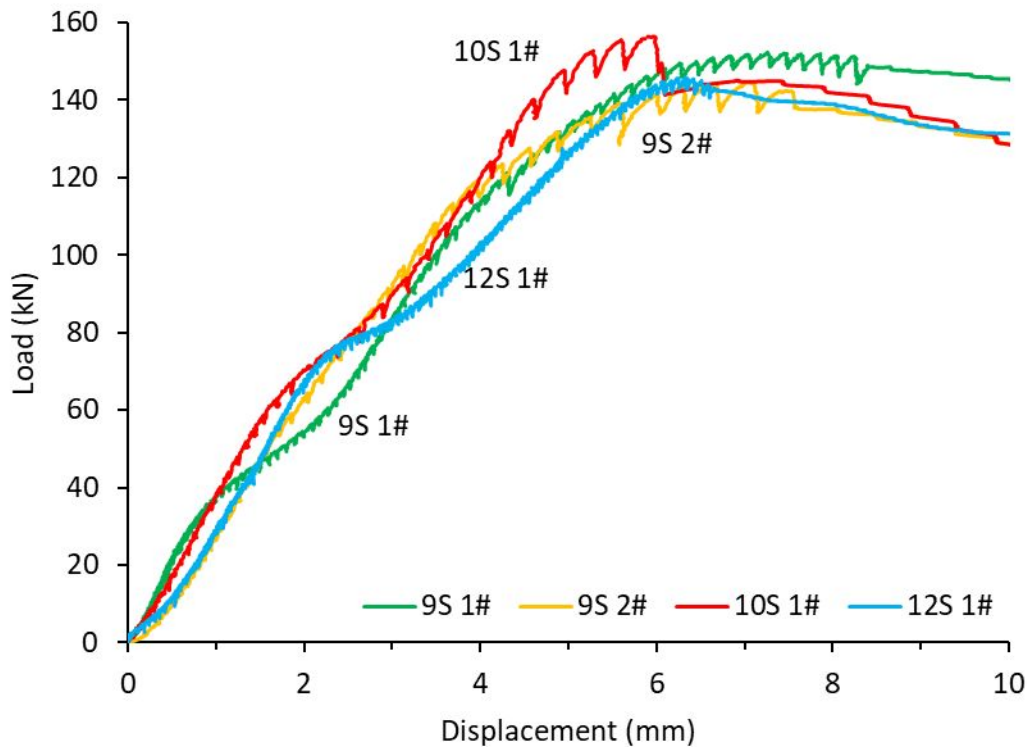


Figure 10 Pre peak monotonic results of 9S, 10S, and 12S bulbed cables

3.2 Cyclic Testing

From the individual cyclic loading comparisons (i.e., Figure 11 and supplementary data), it can be concluded that cyclic loading had no significant adverse loading effect on any of the samples. The results indicate that in the unbulbed cables, the cyclic loading had almost no impact on system behaviour (Figure A3-A5). However, in the bulbed cables, the load increased slightly in the cyclic loading compared to monotonic loading (Figure A6-A8). There may be multiple reasons why this was observed. The fact that this phenomenon is more pronounced in bulbed cables can suggest this may have resulted from the compaction of the failed material in the borehole in between loading and unloading cycles.

Moreover, the results of the cyclic tests (e.g., the 10 strand cable in Figure 11) suggest that the system's initial stiffness was largely unchanged in the cyclic loading pattern. In all cases, the load curve commenced from the origin point of the graph and reached the designated load of the step with a slightly stiffer response compared to the monotonic loading. In the unloading section, the load kept declining as the jack's ram was lowered until the load on the cable was zeroed. The bulbed cables had mostly experienced permanent displacement at this stage, and the plain cables mostly had returned to their original location. In the consequent load steps, even the plain cables (Superstrand, indented Superstrand, and Goliath) underwent irreversible displacements.

In the second loading step, the load pick-up point was at slightly less displacement than the load release point of the previous step (Figure 11). This small difference might relate to the elastic strain of the cable and the cable being pulled back in after the load release in the resettling process. However, considering the loads are relatively low (i.e., minimum elastic strain) and the fact that this phenomenon is more evident in the bulbed cables (9, 10, and 12 strand), elastic strain seems to be the less influential factor. Since bulb structures are curved and larger than the rest of the cable, they tend to settle slightly lower once the load is released, thereby pulling the cable back depending on their position when the load was removed. This explanation can also be valid for the plain cable bolts (especially thicker strand cables) as the spiral nature of a cable provides the same effect, albeit at a much smaller scale.

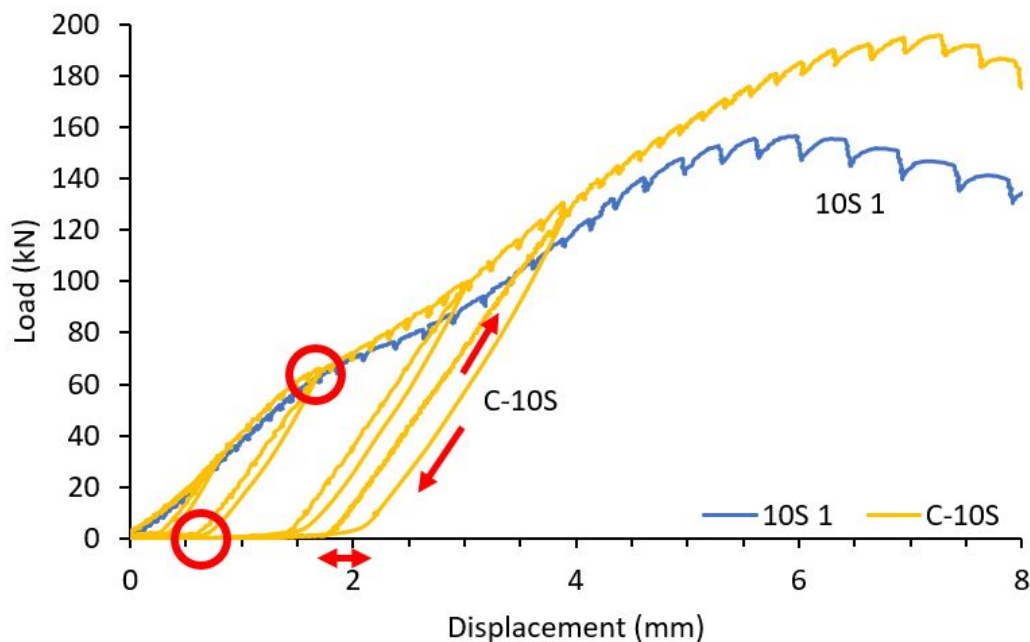


Figure 11 Cyclic and monotonic testing of 10S cable

The cyclic results suggest that resin-anchored cable bolts provide a similar response in a repeated load pattern regardless of how much they have been pulled axially out of their initial position as long as their monotonic load capacity is not reached. This is important as during their service life, cable bolts can undergo stress fluctuations due to mining and non-mining activities. The results suggest that resin-anchored cable bolts can have good recovery and useability even after cycles of loading and unloading which, in the overall scope of underground support design, means more versatility and robustness.

3.3 Discussion

3.3.1 Rotation

After each test, a considerable amount of stored energy was observed on the wings of the anti-rotation plate. When this plate was released, a sudden rotation in the direction of the cable lay occurred. The amount of rotation seems to be related to the total pull out displacement and the cable type rather than the type of loading, as seen in Figure 12.

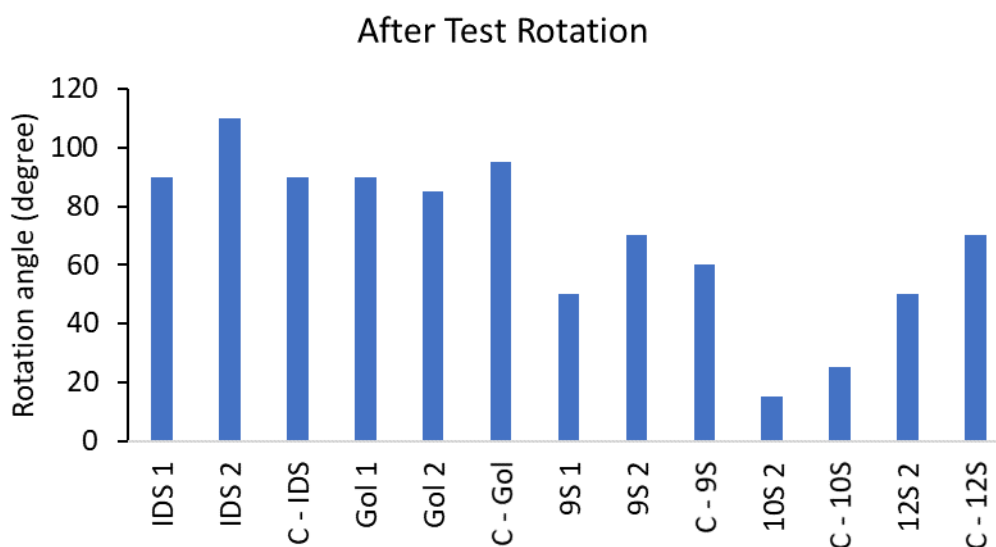


Figure 12 Approximate value of rotation observed when the anti-rotation plate was freed after the tests

The rotation value in Figure 12 is believed to be mainly due to the difference in the rate of rotation between the entry and exit point of the cable relative to the concrete confinement. As the cable is pulled out, inevitably an exposed section of the cable is revealed. This naked section tends to untwist so the strands become straight. Simultaneously, the anchor tube resists the rotational movement, while on the other end, the tendency for the cable to unscrew from the resin is exerting more load. These two forces caused damage zones (approximately 50 mm long) at the top of the resin annulus (exit point) and at the bottom of the anchor tubes, resulting in the exposed length being larger than the pulled out length (Figure 13).

More importantly, as seen in the inspected opened samples after the test, the cable rotation state varies along the encapsulation length. The entry point of the cable (bottom of the concrete sample) completely unscrews without damage to the resin ridges, while at the exit point (top of the annulus) the cable tends to break the ridges due to various mechanisms including untwisting. The total amount of rotation observed in a cable pull out test seems to be inevitable and occurs independently of the anti-rotation mechanism.

The total rotation either happens gradually throughout the test (in a non-rotationally constrained setup) or in a sudden movement when the load is released (in a rotationally constrained setup).

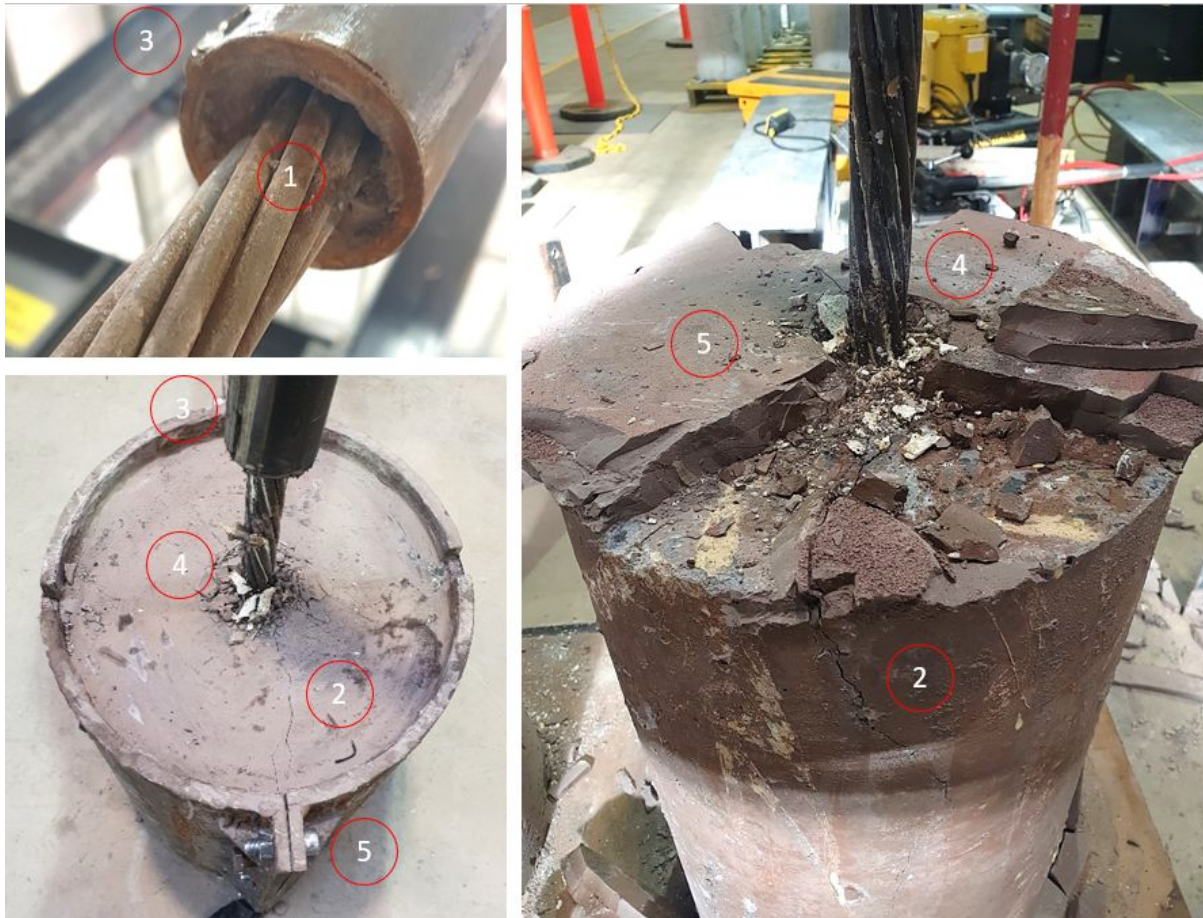


Figure 13 Sample failure: 1. Bottom of anchor tube failure, 2. Radial crack, 3. Anti-rotation key, 4. Top of sample failure, and 5. Top surface confinement with a 70 mm central hole

3.3.2 Oscillations

In all the tests, the residual section of the graph consisted of many small oscillations accompanied by audible breaking noises from the samples (Figure 14). As shown in the graph, during each oscillation, the load increased up to a relatively fixed value, then dropped (with a breaking sound) to another relatively fixed value, and this pattern was repeated. There does not appear to be any connection between these oscillations and the experimental parameters. Post-peak oscillations were also reported in previous studies by Stillborg (1984), Moosavi *et al.* (2005), Martin (2012), Chen (2016), and Li *et al.* (2019).

It was deduced that this section of the graph represents the debonded cable being pulled through the resin column, and the interaction of the strands and the resin ridges (lugs) were the source of the irregularities. However, further investigation revealed the oscillations are far more irregularly spaced (Figure 15) to directly correlate with the cable

strands *jumping* from ridge to ridge. The oscillations were present in both the bulbed and unbulbed cables and the shape of the ridges after the experiment clearly showed they were not broken (sheared off) during the test.

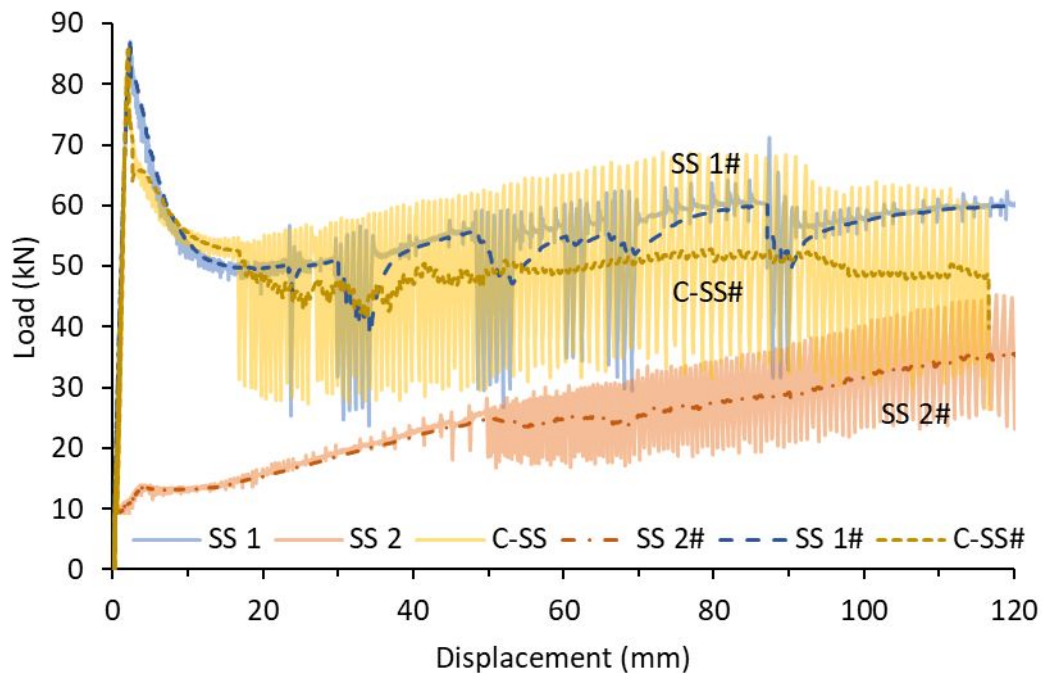


Figure 14 Example of noise and oscillation reduction in the post-peak results

The authors believe a longitudinal and rotational *stick-slip* movement, also identified by Li *et al.* (2019), can explain this phenomenon. The stick-slip phenomenon is similar to an earthquake behaviour, where the stored energy is released in segments as pre/aftershocks rather than through one large de-stressing event. This means that for each increment of the pull out, a specific rotational and axial force is stored in the cable between the deeper and shallower sections of the annulus. When this force reaches a high enough level, the cable pulls out and twists, and the cycle repeats itself. Studying the evidence from the entry point of the cable (bottom of the concrete block) reveals that after each load drop from the upper to lower bound of oscillation, no rotation is observed at the end of the cable. This supports why there were stored rotational forces after the test at the exit point.

It is also important to note that different points of the encapsulation length undergo different axial and rotational loads due to the cable bolts consisting of multiple individual strands/elements. So, it is likely that the rotation along the encapsulation length of the cable is not uniformly distributed. This was later supported by observing the undisturbed edges (ridges) of resin toward the bottom of the holes (Figure 15) in the opened concrete sample. For improved interpretation, the graphs' post-peak data were denoised using an exponential smoothing function with a coefficient of 0.99. The modified values

approximately represent the mean value of the upper and lower band of each oscillation which made the reporting of graphs easier and more comprehensible.

3.3.3 Post Test Sample Inspections

After the test, all the samples were broken in half to investigate the quality of encapsulation and better understand the failure mechanism (Figure 15). In almost all the samples, the following observations can be made:

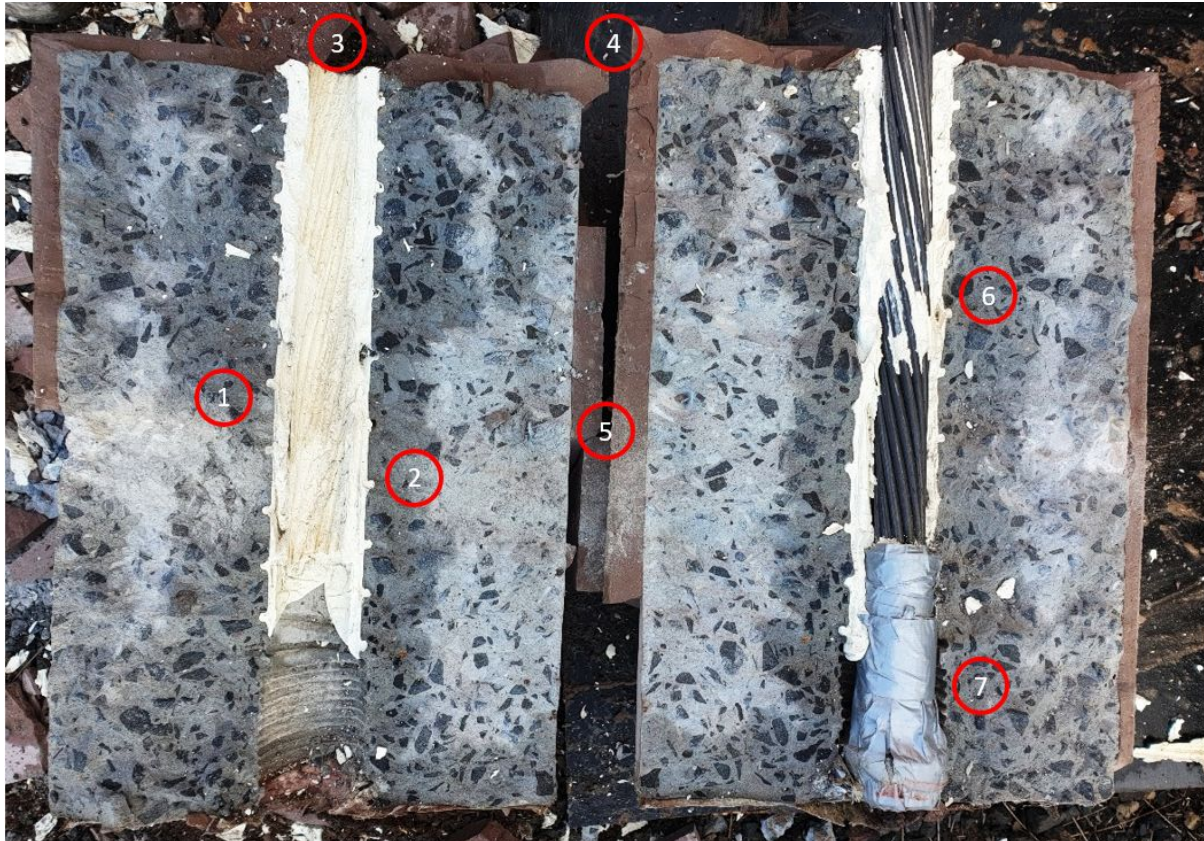


Figure 15 Broken 12S cyclic sample: 1. Riffling, 2. Original location of the bulb, 3. Collar, 4. Surface confinement, 5. Radial confinement, 6. Bulb after the test, and 7. Ungrouted section

- All cables remained firm in place in the annulus even when the samples were broken in half. Cables had to be removed from the resin with considerable force. This indicates that the system possessed significant integrity even after 120 mm of vertical displacement and being broken in half.
- The resin ridges were intact in all samples. This is contrary to the pull out of rock bolts, where the annulus surface is significantly scraped off and damaged by the ribs. It is suggested that the slight relative movements of strands with respect to each other and their unique size and shape, increase the tendency of slips along and in between the ridges. The fact that strands *travel through* the ridges, rather than shearing off, and maintain contact can be potentially useful in design.

- The subtle indentations of the indented Superstrand cable were entirely imprinted on the resin, showing that surface modifications matter and that the viscosity of the bonding agent should be designed to utilise the indentations. The same finding applies to the bulbed cables and how the bulbs were filled (Figure 16).
- As the distance from the borehole collar increases, the ridges are sharper and more pristine. This is a crucial point and supports the notion that load (shear and rotational) distribution along the cable bolt is not uniform, and the majority of the load (hence, most damage) occurs in the vicinity of the exit point (Figure 16). Further away from the collar (toward the entry point), the resin annulus is relatively undamaged.
- It also appears that further away from the collar, the dominant behaviour is unscrewing in a *stick-slip* manner rather than pure vertical movement. This also applies to the cyclic loading behaviour. Videos of the entry point on the bottom of the concrete samples in similar tests show a constant rotation of the end of the cable as it goes into the concrete while the rotation of the exit point at top of the concrete is zero. It should be recalled that the anti-rotation measure is on the anchor tube *outside* the concrete embedment length. So, the further away from the anchor tube, the more the rotational tendencies influence the tests. This is likely why the resin ridges are less damaged towards the end of the resin annulus (on the bottom of the concrete sample) than around the collar (Figure 17).
- Each loading cycle could be considered a new monotonic test. The only difference is that the exposed cable length (between the top of the concrete and the anti-rotation point) increases, and the bonding agent at the cable exit point and the bottom of the anchor tube is damaged. These gradual differences work to increase the rotational tendencies of the cable which add additional complexities in understanding the behaviour of the system.



Figure 16 Top: Indentation imprints of IDSuperstrand cable, Bottom: Broken sample 12S. Dull top and sharp bottom (below the bulb): Left = Collar, Right = Bulb



Figure 17 Broken Goliath cyclic sample - sharper ridges in the bottom and duller towards the collar

4 Conclusions

A systematic experimental study was carried out on resin-encapsulated cable bolts under both monotonic and cyclic loadings using a 1000 kN pull out testing machine. The results of monotonic loading tests suggested that the diameter of the cable was the determining factor in the behaviour of the system. The smaller the diameter, the more

significant variability emerged from the results. The results also showed smaller diameter cables have a higher sensitivity to the resin encapsulation quality. The findings of this study support the role of surface and structural modifications (i.e., indentation and bulbs) in increasing the overall axial load of the system. It was concluded from the broken samples that there is a slight relative rotational stick-slip movement of the cable inside the annulus column.

In the cyclic experiments, the results suggested that a cyclic loading pattern in non-bulbed cables did not have a significant impact whereas, in the bulbed cables, an increased peak load was observed. The cyclic results revealed that plain cables (non-bulbed) tended to have no minimum permanent displacement after each unloading step for the lower loads, whereas bulbed cables tended to have a permanent displacement due to the bulb destroying the resin annulus. Further investigation of the cyclic results showed that the load picks up point is at a slightly lower displacement than the previous unloading section, especially in the bulbed cables.

The broken samples suggested that the type of loading does not change the type of failure observed on the annulus. It was inferred that, as the distance from the exit point increases, the damage decreases. This was especially true for the plain cables. In the bulbed cables, the movement of the bulb tended to scrape more material from the walls. The resin used in this study proved to be viscous and slow setting enough to provide full encapsulation, filling the bulbs, and was embossed by the surface indentations. Most importantly, the results demonstrated that the integrity of the cable bolt system was not adversely affected in cyclic loading. This indicates that cable bolts may be used effectively in complex stress regimes, subject to their monotonic peak load not being violated.

This study can be further extended to investigate the effects of cyclic loading on cementitious grout-encapsulated cable bolts. Although the increasing step loading pattern used in the study provided an appropriate starting point for investigating more complicated loading conditions for the cable bolts and additional scenarios such as reciprocal loading (pull-push) or anisotropic stresses could be explored. Also, a scale dependency study can shine a light on the axial behaviour of the cables in small scale and field scale. Lastly, a comparison between the field pull out tests with the large scale laboratory pull out test on fast-setting cable bolt resins, such as that presented in this study, can be helpful to breach the gap between the research and practice.

5 Acknowledgements

The authors wish to acknowledge the valuable support of Minova and Jenmar who provided the materials necessary to bring this study to fruition. Mr Robert Hawker, Mr Tom Meikle, Mr Peter Craig, and Ms Arya Gao must also be acknowledged for their invaluable in-kind support.

6 Competing Interests

The authors declare there are no competing interests.

7 Data Availability

Data generated or analysed during this study are provided in full within the published article and its supplementary materials.

8 Funding Statement

The authors received no external financial support for the research, authorship, and/or publication of this article.

9 References

- Aziz, N., Majoor, D., and Mirzaghobanali, A. 2017. Strength Properties of Grout for Strata Reinforcement. *Procedia Engineering*, **191**(1): 1178–1184. doi:10.1016/j.proeng.2017.05.293.
- Aziz, N., Mirza, A., Nemick, J., Li, X., Rasekh, H., Wang, G.G., Nemcik, J., Li, X., Rasekh, H., and Wang, G.G. 2016. Load Transfer Characteristics of Plain and Spiral Cable Bolts Tested in New Non Rotating Pull Testing Apparatus. *In Coal Operators' Conference*. Wollongong.
- Bajwa, P.S., Hagan, P., and Li, D. 2017. A comparison between resin and a cementitious material in the grouting of cable bolts. *In Coal Operators' Conference*. Wollongong. pp. 193–203.
- Chen, J. 2016. Load Transfer Mechanism of Fully Grouted Cable Bolts. University of New South Wales.
- Chen, J., Hagan, P.C., and Saydam, S. 2016. Load transfer behavior of fully grouted cable bolts reinforced in weak rocks under tensile loading conditions. *Geotechnical Testing Journal*, **39**(2): 252–263. ASTM International. doi:10.1520/GTJ20150096.
- Chen, J., Hagan, P.C., and Saydam, S. 2018. A new laboratory short encapsulation pull test for investigating load transfer behavior of fully grouted cable bolts. *Geotechnical Testing Journal*, **41**(3): 435–447. doi:10.1520/GTJ20170139.

- Clifford, B., Kent, L., Altounyan, P., and Bigby, D. 2001. Systems used in coal mining development in long tendon reinforcement. *In Proceedings 20th International Conference on Ground Control in Mining*. pp. 7–9.
- Craig, P., and Holden, M. 2014. In situ bond strength testing of Australian cable bolts. *In Coal Operators' Conference*. Wollongong. pp. 147–155.
- Fuller, P.G., and Cox, R.H.T. 1975. Mechanics of load transfer from steel tendons to cement based grout. *In 5th Australian Conference on Structures and Materials*. Civil Engng Departments, Melbourne and Monash University, Melbourne. pp. 189–203.
- Hagan, P., and Chen, J. 2015. Optimising the selection of cable bolts in varying geotechnical environments (C22010). *In ACARP*. Sydney.
- Hawkes, J.M., and Evans, R.H. 1951. Bond stresses in reinforced concrete columns and beams. *Journal of the Institute of Structural Engineers*, **24**(10): 323–327.
- Hutchins, W.R., Bywater, S., Thompson, A.G., and Windsor, C.R. 1990. A versatile grouted cable dowel reinforcing system for rock. *In AusIMM*. pp. 25–29.
- Hyett, A.J., Bawden, W.F., Macsporrán, G.R., and Moosavi, M. 1995. A Constitutive Law for Bond Failure of Fully-grouted Cable Bolts Using a Modified Hoek Cell. *International Journal of Rock Mechanics and Mining Sciences & Geomechanics Abstracts*, **32**(1): 11–36. Elsevier.
- Hyett, A.J., Moosavi, M., and Bawden, W.F. 1996. Load distribution along fully grouted bolts, with emphasis on cable bolt reinforcement. *International journal for numerical and analytical methods in geomechanics*, **20**(7): 517–544.
- Jennmar Australia. 2020. Product Catalogue Coal Mining.
- Kilic, A., Yasar, E., and Celik, A.G. 2002. Effect of grout properties on the pull-out load capacity of fully grouted rock bolt. *Tunnelling and Underground Space Technology*, **17**(4): 355–362. doi:10.1016/S0886-7798(02)00038-X.
- Li, D., Masoumi, H., Hagan, P.C., and Saydam, S. 2019. Experimental and analytical study on the mechanical behaviour of cable bolts subjected to axial loading and constant normal stiffness. *International Journal of Rock Mechanics and Mining Sciences*, **113**(December 2018): 83–91. Elsevier Ltd. doi:10.1016/j.ijrmms.2018.11.011.
- MacSporrán, G.R. 1993. An empirical investigation into the effects of mine induced stress change on standard cable bolt capacity. Queen's University.
- Martin, L.B. 2012. Theoretical and experimental study of fully grouted rockbolts and cablebolts under axial loads. ParisTech.
- Meikle, T., Tadolini, S.C., Hawker, R., and Pollack, D. 2013. Improvements in long tendon support with pumpable resin. *In Coal Operators' Conference*. University of Wollongong, Wollongong. pp. 18–20.
- Minova. 2020. Carbothix. Available from <https://www.minovaglobal.com/apac/solutions/anchoring-grouts/carbothix/>.
- Moosavi, M., Bawden, W.F., and Hyett, A.J. 1996. A comprehensive laboratory test program to study the behavior of modified geometry cable bolt support. *In Rock mechanics tools and*

- techniques. pp. 209–216.
- Moosavi, M., Jafari, A., and Khosravi, A. 2005. Bond of cement grouted reinforcing bars under constant radial pressure. *Cement and Concrete Composites*, **27**(1): 103–109. doi:10.1016/j.cemconcomp.2003.12.002.
- Rasekh, H. 2017. The performance of cable bolts in experimental, numerical and mathematical shear studies. University of Wollongong.
- Rastegarmanesh, A., Mirzaghobanali, A., McDougall, K., Aziz, N., Anzanpour, S., Nourizadeh, H., and Moosavi, M. 2022. Axial Performance of Cementitious Grouted Cable Bolts Under Rotation Constraint Scenarios. *Rock Mechanics and Rock Engineering*, **55**(9): 5773–5788. doi:10.1007/s00603-022-02950-4.
- Reichert, R.D. 1991. A Laboratory and field investigation of the major factors influencing bond capacity of grouted cable bolts. Queen's University.
- Salcher, M., and Bertuzzi, R. 2018. Results of pull tests of rock bolts and cable bolts in Sydney sandstone and shale. *Tunnelling and Underground Space Technology*, **74**: 60–70. Pergamon. doi:10.1016/J.TUST.2018.01.004.
- Stillborg, B. 1984. Experimental investigation of steel cables for rock reinforcement in hard rock. Lulea University.
- Thenevin, I., Blanco-Martín, L., Hadj-Hassen, F., Schleifer, J., Lubosik, Z., and Wrana, A. 2017. Laboratory pull-out tests on fully grouted rock bolts and cable bolts: Results and lessons learned. *Journal of Rock Mechanics and Geotechnical Engineering*, **9**(5): 843–855. Institute of Rock and Soil Mechanics, Chinese Academy of Sciences. doi:10.1016/j.jrmge.2017.04.005.
- Thomas, R. 2012. The load transfer properties of post-groutable cable bolts used in the Australian coal industry. *In Proceedings 31st International Conference on Ground Control in Mining*. pp. 1–10.
- Villaescusa, E., Varden, R., and Hassell, R. 2008. Quantifying the performance of resin anchored rock bolts in the Australian underground hard rock mining industry. *International Journal of Rock Mechanics and Mining Sciences*, **45**(1): 94–102. doi:10.1016/j.ijrmms.2007.03.004.